DEFECT TOLERANCE ANALYSIS OF CRUCIFORM WELDED JOINTS SUBJECTED TO FATIGUE LOADING

J.A. FERREIRA*, C.M.BRANCO** and J.C.RADON***

Defect tolerance curves for non-load carrying cruciform welded joints subjected to fatigue loading in bending were derived using Fracture Mechanics. These curves were compared with the experimental S-N curves obtained from fillet welded specimens of medium strength steel St 52-3 of 12 mm plate thickness. A considerable difference in fatigue life was obtained due to a significant crack initiation period. However good agreement was found with similar data published in the literature.

A defect tolerance procedure was carried out for this type of joints in bending using both classes E and F of the BS 5400 code.

INTRODUCTION

Non-load carrying cruciform welded joints are quite extensively used in welded structures and may be subjected either to axial loading or bending depending on the type of structure concerned. However in design codes such as BS 5400 (1) the design stresses are usually based upon test results obtained under axial loading, which may be unduly conservative for joints loaded in bending. Hence one of the objectives of the work was to obtain S-N data for these joints in bending and compare the results with the appropriate fatigue design curves in the code.

In welded joints crack propagation plays a dominant part in the fatigue life. In non-load carrying joints fatigue cracks usually initiate at the weld toe and propagate through the plate thickness. Fracture Mechanics has been applied sucessfully to describe both crack propagation and fatigue life of welded joints. Several detailed examples are available in the literature (2 to 5) but these are mainly for joints loaded in tension. Bending loading has not often been considered in the Fracture Mechanics studies of welded joints.

The application of LEFM in the fatigue analysis of welded joints is dependent on the availability of stress intensity factor solutions. These solutions should be sufficiently accurate without the need of extensive time spent in data preparation and computer use. In simply shaped welded joints the Albrecht method (6) is often used to compute stress intensity values. The method is easy to apply and does not require a great amount of computer

* Research assistant, University of Coimbra, Coimbra, Portugal
** Professor, University of Minho, Largo do Paço, Braga, Portugal
*** Research fellow, Imperial College, London, England

time or memory. For practical purposes the method is accurate enough provided a basic stress intensity factor solution is known and the stresses can be computed with a good degree of accuracy. Basically the method consists of calculating the stress intensity factor K in the welded joint using the equation

$$K = K^1 F_G \quad (1)$$

where K^1 is the stress intensity factor solution assuming a uniform stress distribution in the crack propagation line and F_G is a dimensionless factor which takes into account exclusively the non-uniform stress distribution in the weldment. If K^1 is known for a similar geometry and loading mode without the weld, F_G can be computed using an equation derived by Albrecht (6) and based on the stress values computed along the crack line.

The stresses required for the determination of F_G can be conveniently computed using the finite element method. Various types of elements may be used, here, namely, the constant strain triangular element, the eight node isoparametric element and also 3D elements. Most of K solutions available in the literature were obtained for joints loaded in tension using triangular elements (7). The authors have carried out an extensive computation of stress intensity factors in non load carrying cruciform fillet welded joints loaded in bending and tension (8). The eight node 2D isoparametric element was used and the results allowed an assessment of the influence of the loading mode and weld geometry parameters such as plate length, weld penetration, plate thickness, attachment plate thickness weld angle and weld leg length, on the stress distribution and on the stress intensity factors. Some of the results were compared with those available in the Literature and good agreement was found.

In this paper the above mentioned K results are applied in the defect tolerance analysis in fatigue loading using both classes E and F curves of the BS 5400 design code. S-N crack propagation curves are obtained as a function of initial flaw sizes together with other appropriate curves relating nominal stress, initial flaw size, plate thickness, weld and plate geometry with the fatigue life. Finally S-N data are presented for non load carrying cruciform welded specimens of steel St 52-3 loaded in cantilever bending. These experimental data are compared with other results available in the literature and also with the theoretical S-N curves.

STRESS INTENSITY FACTOR COMPUTATION

The details of the computation and all the stress concentration and stress intensity factor results may be found in (8) and (9). Here only the most important points of the analysis will be mentioned. Figure 1 shows the finite element mesh for the full penetration non load carrying cruciform weld, and Figure 2 is the specimen sketch with the nomenclature used in the analysis of the weldment with the more important parameters of the joint identified. Thus in Fig.2, B is the main plate thickness, B_1 is the attachment plate thickness, LG is the weld leg length and θ is the weld angle measured from the weld toe.

A comparative study carried out at an earlier date and using a coarser mesh showed that both the weld penetration and the plate length (L, see Fig.1) affected the stress distribution only by 1 to 2%(9). Hence it was decided to use the mesh size shown in Fig. 1 since a good correlation was obtained with the numerical and analytical solutions used as test cases. This mesh was not refined any further since an increasing number of elements would have exceeded the available computer facilities.

Two loading modes were considered: a uniform tension and cantilever bending both applied through the main plate of the weldment. Uniform tension was achieved applying a uniform load distribution along the 169 to 177 node line (Fig. 1). Cantilever bending was simulated, constraining the vertical and horizontal displacements in the far left vertical line (nodes 1 to 9) and applying a vertical concentrated load in node 172 (Fig.1).

The stresses were obtained at the Gauss integration points of the isoparametric elements and along lines 1 and 2 shown in Fig. 2. The crack was assumed to propagate from the weld toe along line 1 in the thickness direction. Hence stress distribution plots were obtained along lines 1 and 2 and from those the values of the stress concentration factor at the weld toe, K_t, were derived (point A in Fig. 2). The values of the parameters used in the K_t and K calculations are given in Table 1 (8). These values were selected because they represent typical values in welded structures and cover a wider range of weld details than those usually quoted in the literature.

TABLE 1 GEOMETRICAL PARAMETERS OF THE WELDED JOINTS (8)

B (mm)	B_1 (mm)	LG (mm)	θ	B (mm)	B_1 (mm)	LG (mm)	θ
4	10	5	26.57	24	10 and 20	5	63.43
12	10	5	26.57	48	10 and 20	5	63.43
4	10	5; 2.5 and 10	45	24	10 and	2.5 and 10	45
12	10	5; 2.5 and 10	45	48	10 and	2.5; and 10	45
4	10	5	63.43	24	10 and 20	5	45
12	10	5	63.43	48	10 and 20	5	45

F_G values in equation 1 were obtained by applying the appropriate expression used in (6). The F_G factor will now be called M_K, to comply with the notation commonly used for welded joints (7). As mentioned in the Introduction the F_G calculation is based on the computed stress values along the crack line (Fig. 2). Hence M_K values were obtained as a function of (a/B), and it was found that a power law correlation fitted rather well with the results and was given by the equation

$$M_K = p/(a/B)^q \quad (2)$$

where p and q are constant functions of the loading mode and of the weld and plate geometry (B, B_1, LG and θ). The complete set of M_k values may be found in (8). A typical plot of M_k against a/B is shown in Figure 3 for a joint where θ=45°, B = 12 mm and B_1 = 10 mm. M_k decreases as the crack ratio a/B increases and approaches the value 1 for a/B values close to 0.1. Also it is seen that M_k increases with the weld leg length, but only with a minor increase for bending. No influence of weld leg length was noted for a/B values greater than 0.05. Figure 3 results also show that M_k is greater in tension than in bending and this difference increases as a/B increases.

The main conclusions of the stress intensity factor computation (8,9) are summarized below

(i) In cantilever bending K values are 20 to 30% less than in tension

(ii) K increases with the main plate thickness. However only a very small increase was observed for small values of the ratio LG/B and B_1/B

(iii) K increases with both weld leg length and weld angle, but only a slight increase was obtained when the attachment plate thickness was increased

(iv) For a/B values greater than 0.12 in bending and 0.2 in tension M_k values are very close to 1 and hence $K=K^1$

The resulting equations of the stress intensity factor for tension and cantilever bending are as follows:

$$K = (1.122 - 0.569\alpha - 0.205\alpha^2 + 0.471\alpha^3 - 0.19\alpha^4)\ p/(a/B)^q \sigma\sqrt{\pi a} \qquad (3a)$$

$$K = (0.862 + 0.619\alpha + 0.786\alpha^2)\ p/(a/B)^q\ \sigma\sqrt{\pi a} \qquad (3b)$$

where α = a/B and σ is the nominal stress at the weld toe cross section (line 1 in Fig.2). In these equations the terms in brackets are the geometrical factors Y for the K' equations which were taken from the Tada et al (10) solution for a finite plate in tension with an edge crack and the Murakami (11) solution for cantilever and plane bending of a rectangular cross section bar with an edge crack.

DEFECT TOLERANCE ANALYSIS

Variation of initial crack size and design stress with plate thickness

Curves of initial crack size a_i vs. main plate thickness given as function of stress and weld geometry, are very useful if any defect tolerance analysis is to be carried out. These curves were obtained integrating the Paris law of the material and keeping the fatigue life constant. It is well known that this integration for R=0 gives

$$N_r = \int_{a_i}^{B} \frac{da}{C(M_k\ Y\sigma_{max}\sqrt{\pi a})^m} \qquad (4)$$

where N_r is the fatigue life in crack propagation and C and m are respectively the constant and the exponent in Paris law equation. To obtain plots a_i against B, both N_r and σ were kept constant in the integration of equation (4). Thus for N_r a design fatigue life of 2×10^6 cycles was chosen, and σ was the stress at that fatigue life for both mean design curves of classes E

and F of the BS5400 code. These classes were selected since the non load carrying cruciform weld detail in bending can be classified either as class E or F. The values of m = 3.1 and $C = 1.33 \times 10^{-13}$ [Nmm$^{-3/2}$, mm/cycle] are those obtained in previous fatigue crack propagation tests (12) and are in agreement with the usual values for weldable low-alloy steels. In equation (4) the geometrical factor Y was taken from equation 3b. No correction for elliptical crack fronts was needed (Ø = 1) since the fatigue tests have shown that the cracks propagated with values of the ratio (a/2c) between 1/8 and 1/10.

The plots a_i against B are shown in Figures 4 a) to c). They were obtained from the a_i results in equation (4) using also the appropriate values of B (Table 1), and M_k (8,9). Fig. 4 a) results are given as a function of LG (Table 1) keeping both B_1 (10 mm) and θ (45°) constant. In Fig. 4 b) θ is the parameter (Table 1) for a constant value of B_1 = 10 mm, while in Figure 4 c) B_1 is the parameter for constant values of θ = 45° and LG = 5 mm. In Figure 4 c) the defect tolerance curve is plotted for a plate specimen without a weld (B =0). As expected this curve is considerably above the curves for the welded specimens. All these results indicate that defect tolerance levels for class F details are considerably above class E, and this is due to the lower stress values of the class F curve. Figure 4 a) shows that defect tolerance increases when the weld leg length decreases from 10 to 2.5 mm. A considerable variation was found for thicknesses above 12 mm in the class E stress values. For the class F stress no influence of weld leg length was found for thicknesses below 12 mm and only a smaller variation than in the class E was found for thicknesses above 12 mm. Defect tolerance levels in these joints for the class E stress are very low (between 0.1 and 0.001 mm).

The weld angle θ is the main parameter in the defect tolerance curves as shown in Fig. 4 b) when compared with Figs. 4 a) and c). Defect tolerance increases when the weld angle decreases, specially so for thicknesses above 12 mm. The attachment plate thickness B_1 has little influence on defect tolerance as shown by the results in Fig. 4 c). A small increase in defect tolerance can be detected when the attachment plate thickness decreases from 20 to 10 mm but again only for thicknesses above 12 mm.

The initial crack size values or defect tolerance limits, found for the class F stress ranged between 0.1 and 0.5 mm; these are typical flaw sizes in low quality welded joints. Hence cruciform non load carrying joints in bending may be treated as class F details. However a more detailed analysis should consider the variation of the stress for $N_r = 2 \times 10^6$ cycles with plate thickness B for a specific constant value of a_i. The (σ,B) plot is presented in Figure 5 for a value of a_i = 0.2 mm. This value of a_i was selected since it is the most commom flaw size found in welded joints as confirmed by many experimental observations (2). Hence a comparison of results can be made.

The points in Fig. 5 were obtained by solving equation (4) for the stress and the straight lines are the best fit linear regression equations. Each line is for a particular set of parametes LG, θ and B_1 (Table 1) of the curves plotted in Figs. 4 a) to c). It is seen that the stress decreases when the plate thickness B increases. The lowest stress values are for the solution where K reaches the maximum value (LG = 10 mm; θ = 45°, and B_1 = 10 mm) and the highest stress values are straight line Nº5, where K is at the minimum (minimum value of M_k) and those values are for (LG=5 mm; θ = 26°, 57 and B_1 = 10 mm). Hence, using the plot in Figure 5 the stress values can be selected for a certain initial flaw size, weld and plate geometry. For exemple, in Fig.5 the design stress value of the class F curve is indicated and that meets only line Nº5 for thicknesses values close to 48 mm. Therefore this value of design stress (95 MPa) can be assumed to be the lower limit of

stress for cruciform non-load carrying welded joints loaded in bending and can be used safely in the fatigue design of this type of joint . The class E stress (120 MPa) lies outside the range of this 0.2 mm plot as expected from the results plotted in Fig. 4.

A comparison between the lowest σ,B curve (line N95 in Fig. 5) with the experimental results taken from the S-N curves proposed by ESDU (13) for similar joints is presented in Figure 6.The class F design stress lies at the intersection of the two curves for a thickness value of about 40 mm and for class E the intersection point is at 30 mm thickness,but only in the ESDU line. For lower thickness values higher design stresses can be used in bending. The same conclusion may be taken comparing the mean class F and class E design curves with the range of S-N curves proposed by ESDU (Figure 7).

Theoretical S-N crack propagation curves

Equation 4 can be expressed also as an S-N crack propagation curve function of the initial flaw size. This is another way of obtaining defect tolerance results and getting the data presented in Figs. 4 and 5. For an S-N curve, equation (4) becomes

$$\sigma^m N_r = \frac{1}{C} \int_{a_i}^{B} \frac{da}{(M_k Y \sqrt{\pi a})^m} = \frac{I}{C} = \text{const.} \qquad (5)$$

where I is the crack propagation integral. I is constant if a_i and B are kept constants. Equation (5) was solved by numerical integration after substituting the appropriate values of M_k and Y. The curves were obtained for all the geometries defined in Table 1 and Figure 8 presents the set of curves in cantilever bending for B = 12 mm; θ = 45°; LG = 5 mm and B_1 = = 10 mm. It will be seen that the S-N curve is strongly dependent on the initial flaw size with a range of about two orders of magnitude in fatigue life for a_i values between 0.012 mm (0.01 B) and 2.4 mm (0.2 B)

Figure 9 shows the band of S-N curves in cantilever bending for the thickness of 24 mm and for a_i values of 0.012 mm (0.005 B) 0.2 mm and 0.6 mm (0.025 B). Each band is defined by the maximum and minimum S-N curve obtained for these a_i values with the same values of θ, B_1 and LG as given before. The experimental curve proposed by ESDU (13), to fit the results in bending of non-load carrying cruciform joints with 25 mm thickness,is also shown in Fig. 9 for comparative purposes. The slope of the ESDU experimental curve is less than the theoretical curves,due to the crack initiation period which is not taken into account in the theoretical analysis. However a good agreement is obtained for a_i values between 0.2 and 0.6 mm but only in the region where $N_r < 10^5$ cycles. In that region the crack initiation period is very small and therefore the model gives good results,bearing in mind that in welded joints flaws are usually present at the weld toe with dimensions between 0.2 to 0.5 mm (14). For N_r values above 10^5 cycles an accurate prediction of the crack initiation period is necessary before any conclusions can be put forward.

S-N DATA IN CRUCIFORM NON-LOAD CARRYING JOINTS IN BENDING

S-N tests were carried out in cantilever bending in specimens provided with cruciform non-load carrying fillet welded joints. The material selected was a low carbon medium strength steel St 52-3 according to DIN 17100 specification. The chemical composition and principal mechanical properties are given in Table 2.

TABLE 2 - COMPOSITION AND MECHANICAL PROPERTIES OF St 52-3 STEEL

Chemical composition (% in weight)

C - 0.22; S_i -0.55; Mn - 1.50; P - 0.045; S - 0.045

Mechanical properties

σ_{UTS} = 550 MPa ; σ_{ys} = 360 MPa ; ε_R = 18,5 % ;Hardness= 81 HRB

The welds were made by the manual MIG process without stress relieving treatment. Hardness measurements were taken in all the specimens, on the base metal, weld metal and HAZ. Macrosections of all the joints were taken and these were used for the hardness measurements. In some specimens after the fatigue tests,the area where the crack propagated was polished and etched and the microstruture near the crack faces observed. It was found that the crack initiated at the weld toe in the HAZ. Crack propagation was mainly transgranular, initially through the HAZ, and then in the base metal in a direction normal to the bending stress.

The specimens were of the type shown in Fig.2 with B= 12 mm; LG = 5 mm; θ=45° and B_1 = 10 mm. The specimen length taken from the built-in end up to the point of load application, varied between 200 and 250 mm and the width was 40 mm. The fatigue tests were performed in a specially designed test rig at R=0 and 0.4 in air at a frequency of 1410 cycles / min. The nominal stress was monitored during the tests using strain gauges bonded at a location 10 mm away from the weld toe where the crack was going to propagate(weld toe closest to the built-in end). Fatigue crack tip marking was done in all the tests using marking ink. The first marking was done in the early stage of crack growth as soon as the crack became visible. A typical macrophotograph of one fracture surface is shown in Figure 10. It is seen that the crack initiated at the center of the specimen and propagated through the thickness. Semi-eliptical shallow cracks, such as the one shown in Fig. 10, were usually observed right from the early stages of crack growth. The ratios 2c/a varied between 8 and 10 as refered to before, and hence the correction for a non-uniform crack front was not necessary.

The S-N curve for R=0 is plotted in Fig. 8 for comparison with the defect tolerance results. The results for R=0.4 are also plotted and these are below the S-N curve. Hence fatigue life in these joints is influenced by mean stress, specially in the high cycle fatigue region ($N_r > 10^6$ cycles) where endurance decreases by a factor of 3 when the stress ratio increases from 0 to 0.4. This stress ratio effect may be due to the fact that the specimens had no stress relieving treatment after welding. Further tests are necessary to confirm these results.

The experimental S-N curve lies above the theoretical curves and has a lower slope. The difference is due to the crack initiation period of the fatigue tests which was not taken into account in the theoretical analysis. The crack initiation period increased as the stress decreased and this is in agreement with the results plotted in Fig. 8. Hence a suitable crack initiation model should be developed and confirmed by experimental results.

Good agreement was obtained between the S-N curve and the S-N curves proposed by ESDU (13). Fig. 7 shows the S-N curve obtained in these fatigue tests near the ESDU S-N curve for a thickness of 15 mm and having the same slope.

As seen in Fig. 8,both class F and E design curves lie below the expe-

rimental curve. The class F curve came close to the 0.3 mm initial flaw size curve and class E close to the 0.012 mm curve. For the thickness of 24 mm class F curve is in the lower limit of the band of results for a_i = 0.2 mm (Fig. 9) while class E is again close the band for 0.012 mm. Hence for good quality welds (i.e. with grinding treatment to have very low initial flaws) and thicknesses below 24 mm the use of class F design curve leads to very conservative stresses for the plane loading conditions. In this case either the design curves proposed by ESDU or preferably class E curve may be used. However if the plate thickness is above 24 mm the class F design curve should be used irrespective of the quality of the weld. However it is recommended that for low quality welds and lower thicknesses, the class F should be also used since stress ratio effects and high distribution of flaws will be taken into account.

CONCLUSIONS

1. Fracture mechanics can be used in the defect tolerance analysis of non-load carrying cruciform welded joints subjected to fatigue loading.

2. Plate thickness, weld leg length and weld angle were found to be the most important parameters in a defect tolerance analysis of these joints.

3. Good agreement was found between experimental S-N curves obtained in the type of joints mentioned in 1 loaded in cantilever bending, and results published by ESDU.

4. Theoretical S-N crack propagation curves obtained as a function of initial flaw sizes did not agree with the experimental ones due to a significant crack initiation period.

5. For good quality welds and plate thicknesses below 24 mm, class E fatigue design curve of the BS 5400 code may be applied in the fatigue design of cruciform non-load carrying fillet welds subjected mainly to plane bending. However for plate thicknesses above 24 mm or for low quality welds, irrespective of thickness, class F design curve should be used for the same type of joints.

6. Further work should cover a detailed study of crack initiation and also be extended to other types of details in bending.

ACKNOWLEDGEMENTS

The authors wish to acknowledge the finantial support given by AGARD under the P17 ASP 13 research project entitled Development of Damage Tolerance Methods. Some of the fatigue tests were prepared and conducted by Mr. Pedro Matos to whom the authors acknowledge the help.

REFERENCES

1. BS 5400, Part 10, Fatigue design of metallic bridges, British Standards Institution, England, (1980)

2. Gurney, T.R., Fatigue of Welded Structures, (Cambridge University Press, England, 1979)

3. Burdekin, F.M., Fracture mechanics and its application to welded structures, John Player Lecture, Inst.Mech.Eng., London, UK, (1981)

4. Mitsui, Y. and Kurobane, Y., Evaluation of bending fatigue life for fillet welded joints and application to fatigue analysis of tubular joints, Rep. Com. XIII- 1091-83, IIW, 1983

5. Lieurade, H.P., Application of fracture mechanics to the fatigue of welded structures, Rep. Com. XIII - 1074-82, IIW, IRSID, France, 1982

6. Albrecht, P. and Yamada. K., "Rapid calculation of stress intensity factors", J. Est. Div., Proc. ASCE, 103 (ST2), (1977), 77

7. Gurney, T.R., and Johnston, G.O., "A revised analysis of the influence of toe deffects on the fatigue strength of transverse non-load carrying fillet welds, Weld. Res. Int., 9, Nº3, (1979), 43

8. Branco, C.M., Ferreira, J.A. and Radon, J.C., "Calculation of stress intensity factors in welded joints", in Fracture Mechanics Technology, North Holland, 1984, in print.

9. Ferreira, J. and Branco, C.M., A finite element analysis of cruciform welded joints in tension and in bending (in portuguese), 3rd Portuguese National Congress on Applied Mechanics, Lisbon, Portugal, 1983

10. Tada, K., Paris, P.C. and Irwin, G.R., "The stress analysis of cracks handbook", Del Research Corporation, USA, (1973)

11. Murakami, Y., Analysis of mixed mode stress intensity factors by body force methods, in Numerical Methods in Fracture Mechanics, Ed. D.R.J. Owen and A.R. Luxmoore, Pineridge Press. England, 1980

12. Branco, C.M., "Fatigue test results in bending in the St 52-3 steel", Internal report, University of Minho, Portugal, 1983

13. ESDU, Fatigue strength of transverse fillet welded joints and attachments in steel under bending loading, Engineering Science Data Unit, Doc. 78023, London, England, (1978)

14. Signes, E.G. et al, Factors affecting the fatigue strength of welded high strength steels, Brit.Weld. J., 14 (3), (1967), 108

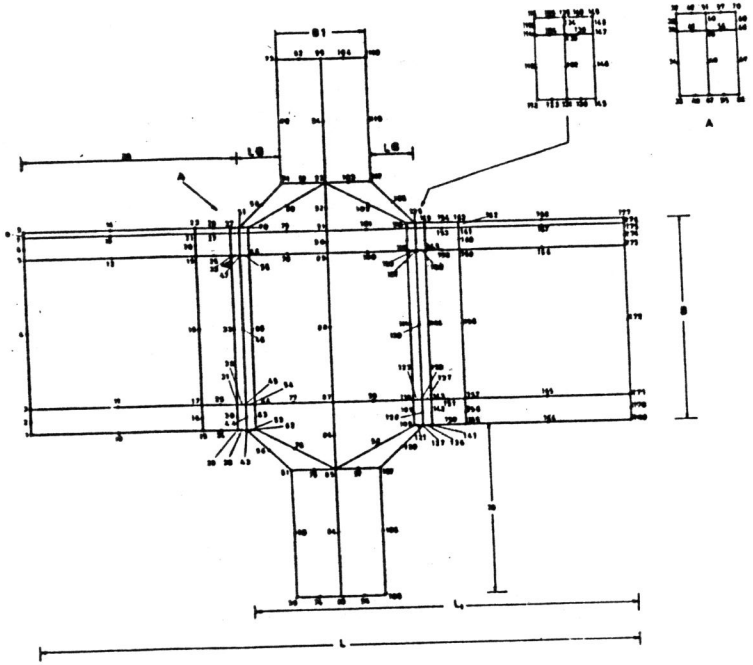

Figure 1. Finite element mesh used in the stress analysis of the cruciform joint (2D isoparametric elements)

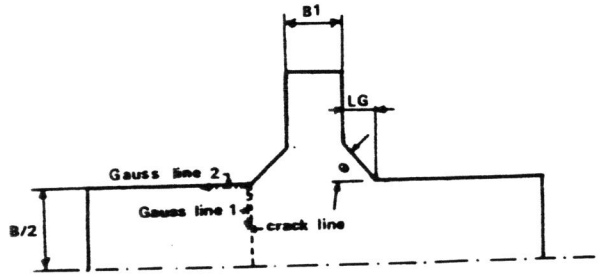

Figure 2. Nomenclature in the weld specimen(non-load carrying cruciform joint)

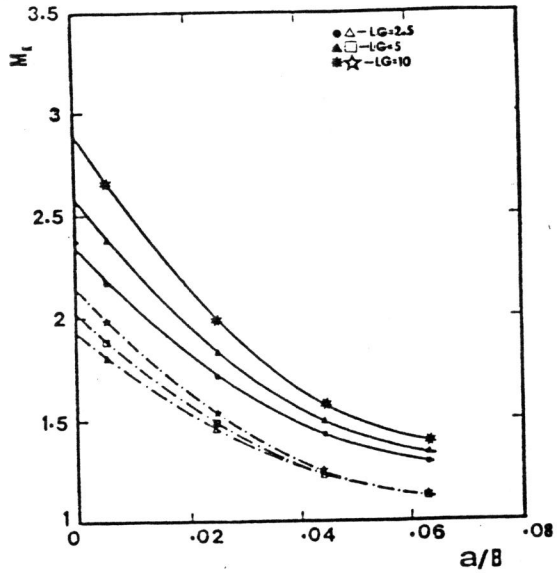

Figure 3. M_k against a/B as a function of LG in tension and cantilever bending.θ=45°. B=12 mm. B_1=10 mm ——— tension; —·—·—·— Bending

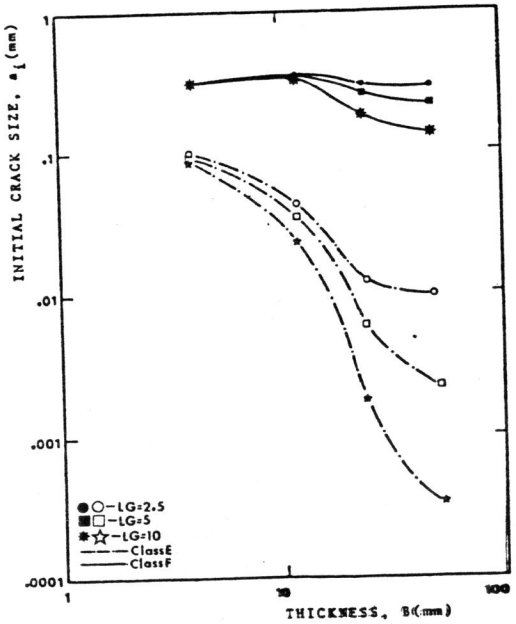

Figure 4. Initial crack size against thickness B. $N_r=2x10^6$ cycles.Cantilever bending.Class E and F stress values
a) Influence of LG for θ=45° and B_1=10 mm

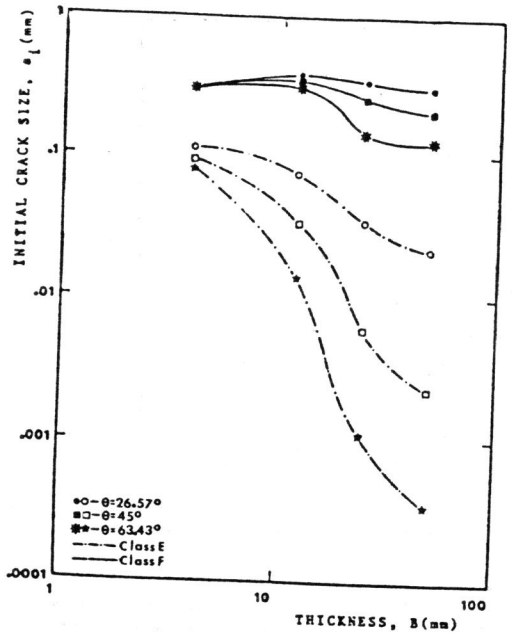

Figure 4. Initial crack size against thickness B. N_r=2x10^6 cycles. Cantilever bending. Class E and F stress values
b) Influence of θ for LG = 5 mm and B_1 = 10 mm

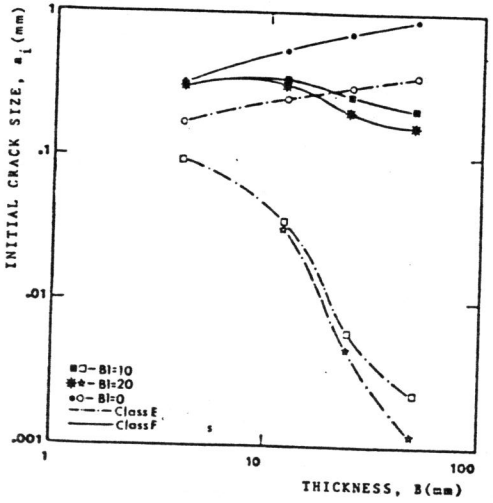

Figure 4 Initial crack size against thickness B. N_r = 2x10^6 cycles. Cantilever bending. Class E and F stress values
c) Influence of B_1 for θ= 45° and LG= 5 mm

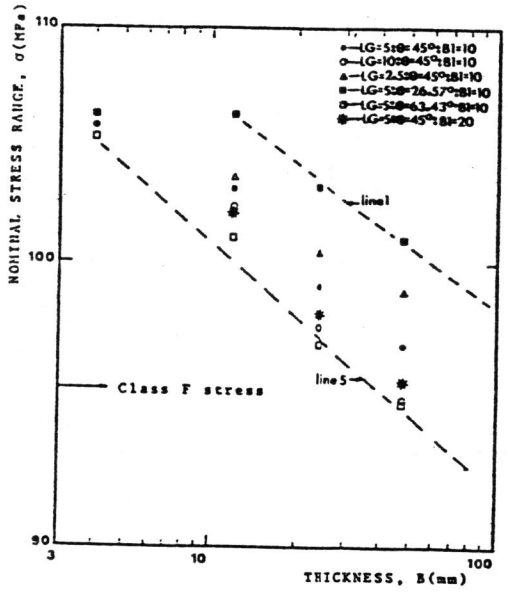

Figure 5 Nominal stress range against plate thickness B. N_r = 2x10^6 cycles. a_i = 0.2 mm. Cantilever bending

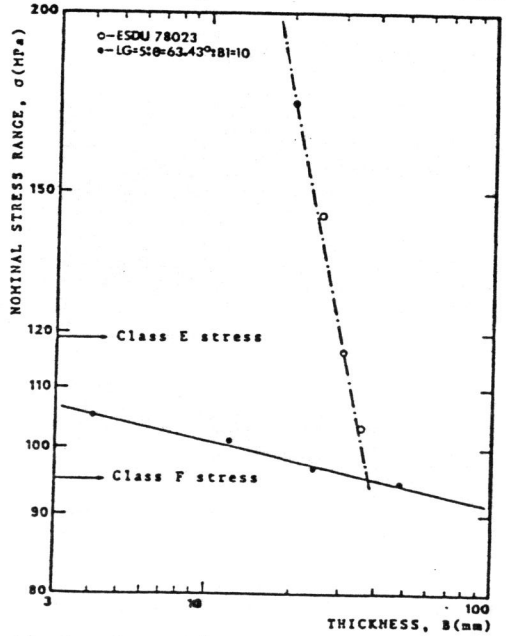

Figure 6 Theoretical and experimental curves, nominal stress range against plate thickness B. N_r = 2x10^6 cycles. Cantilever bending

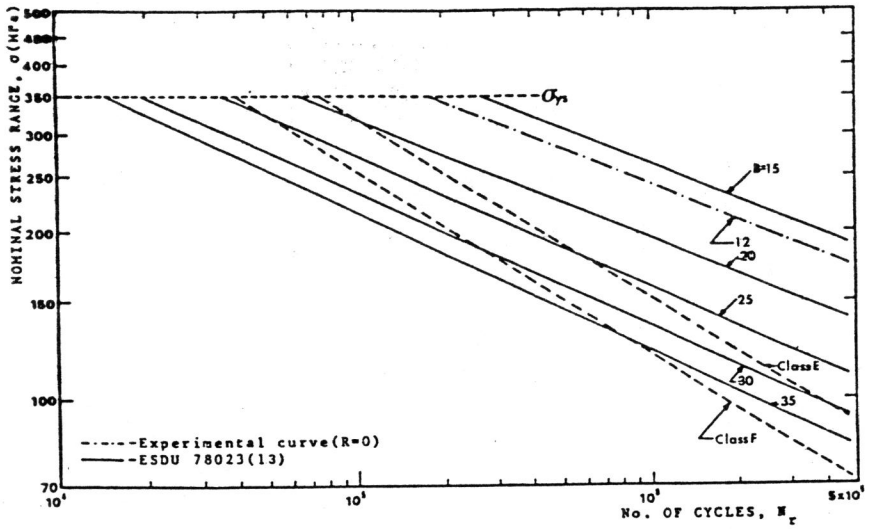

Figure 7 Classes E and F design curves in the BS 5400 code and ESDU S-N curves in bending

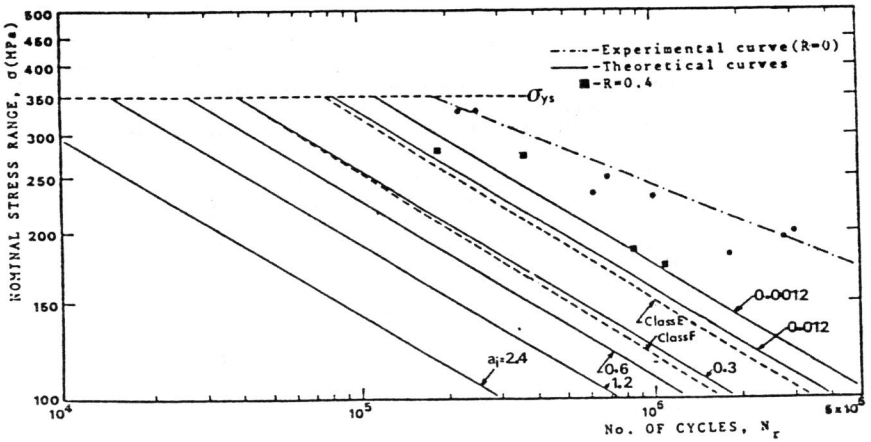

Figure 8 Experimental S-N curve of the St 52-3 steel. S-N crack propagation curves for non-load carrying cruciform joints (B=12 mm; θ=45°; LG=5 mm; B_1= 10 mm). Cantilever bending. R=0

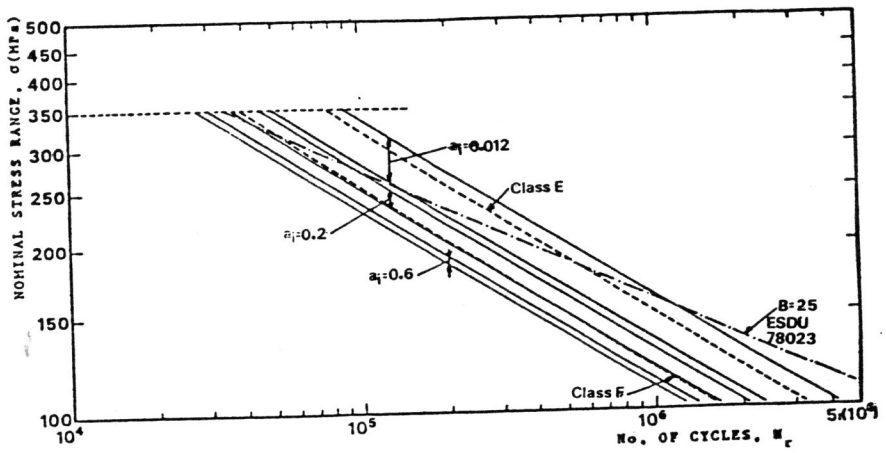

Figure 9 Theoretical S-N crack propagation bands for the thickness of 24 mm. Non-load carrying cruciform joints. Cantilever bending

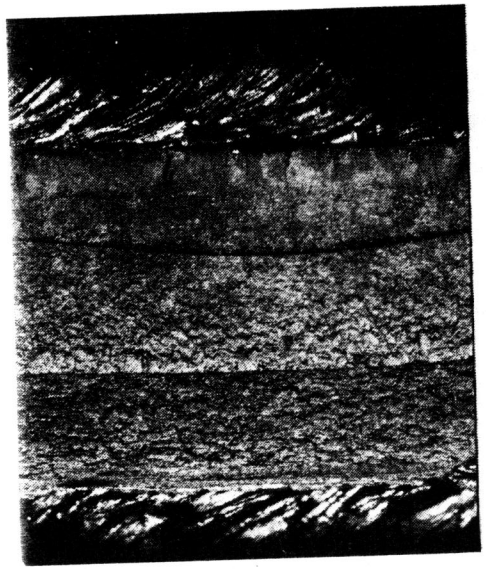

Figure 10 Fracture surface of one fatigue specimen showing shallow crack propagating from the weld toe (Magnification 5X)